

Document Version

Final published version

Licence

Dutch Copyright Act (Article 25fa)

Citation (APA)

Ibrahim, M. S., Poliotti, M., Yang, Y., & Hendriks, M. A. N. (2024). Experimental results of Delft blind prediction contest on shear behaviour of continuous precast girders. In G. L. Balázs, S. Sólyom, & S. Foster (Eds.), *15th PhD Symposium in Budapest-Hungary (2024) – Proceedings: Proceedings of the 15th fib International PhD Symposium in Civil Engineering - 28-30 August 2024 - Budapest, Hungary* (pp. 59-66). fib. The International Federation for Structural Concrete.

Important note

To cite this publication, please use the final published version (if applicable).
Please check the document version above.

Copyright

In case the licence states “Dutch Copyright Act (Article 25fa)”, this publication was made available Green Open Access via the TU Delft Institutional Repository pursuant to Dutch Copyright Act (Article 25fa, the Taverne amendment). This provision does not affect copyright ownership.
Unless copyright is transferred by contract or statute, it remains with the copyright holder.

Sharing and reuse

Other than for strictly personal use, it is not permitted to download, forward or distribute the text or part of it, without the consent of the author(s) and/or copyright holder(s), unless the work is under an open content license such as Creative Commons.

Takedown policy

Please contact us and provide details if you believe this document breaches copyrights.
We will remove access to the work immediately and investigate your claim.

Experimental results of Delft blind prediction contest on shear behaviour of continuous precast girders

Mohammed S. Ibrahim¹, Mauro Poliotti¹, Yuguang Yang¹, and Max A.N. Hendriks^{1,2}

¹*Faculty of Civil Engineering and Geosciences, Delft University of Technology, Stevinweg 1, 2628 CN, Delft, the Netherlands*

²*Department of Structural Engineering Norwegian University of Science and Technology (NTNU), Rich. Birkeland vei 1A, 7491 Trondheim, Norway*

Summary

Precast girders are mainly used as a simply supported system to build multi-span bridges. Alternatively, the precast girders can be made continuous at the intermediate support using cast in situ topping and cross beams. In the Netherlands, a substantial number of these bridges were designed and constructed in this way by following the design regulations in the past. When they are reassessed using Eurocode and the Guidelines for Assessment of Existing Bridges (RBK) by the Rijkswaterstaat (Dutch Ministry of Infrastructure and Water Management), their shear capacity turns out to be insufficient. Since almost no experimental data are available in the literature that can justify the code prediction for this bridge type, a dedicated experimental program has been established to investigate the actual shear behaviour. As a part of this program, this study presents the experimental observation of two full-scale 15 m long shear tests that were part of the recent blind contest at the Delft University of Technology. Using the experimental observations, the predictions of RBK, Model Code, and FprEN 1992-1-1:2023 (Draft for the 2nd generation of Eurocode 2) are examined. The comparison of the codes against the test shows safe and over-conservative predictions for both empirical and strain-based approaches.

1 INTRODUCTION

A century-spanning research on shear has resulted in modern concrete standards[1,2] with stringent requirements that allow consistent design and detailing of bridges and infrastructures. However, applying these standards to assess existing bridges, which now carry heavier traffic loads, often presents significant challenges. This is particularly critical for countries like the Netherlands, where there is a large inventory of concrete bridges that were constructed before the introduction of the current regulations. When assessed via current codes, these bridges often have insufficient shear reinforcement and do not satisfy strength requirements. Despite this, the bridges are handling current traffic, and no incidents have been reported yet. In recent years, to improve assessment strategies and address these conundrums, a series of proactive investigations into various types of bridges were conducted [3–7]

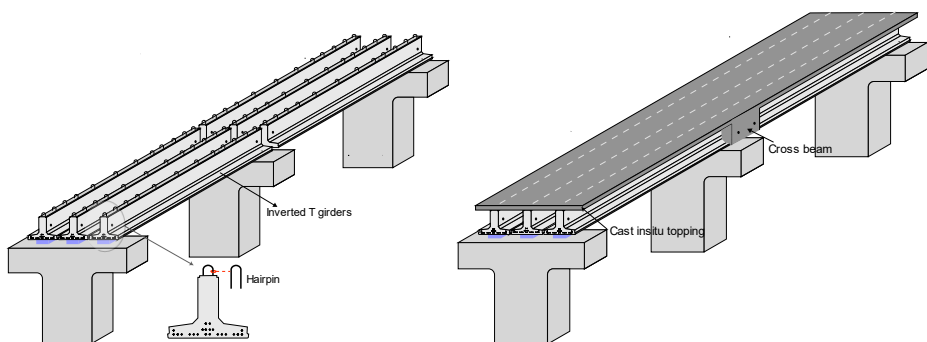


Fig. 1 Construction process of precast continuous girder

Recently, concerns have been raised about a bridge system widely used since the 1950s. The bridge system comprises precast inverted T-girder elements connected at the intermediate support using cast in situ concrete and cross beams. Figure 1 illustrates the construction process of a typical precast continuous bridge. The bridge system provides continuity at the intermediate support and offers several benefits, including reduced sagging moments, better riding comfort, and possible redistribution in case of overloads. This advantage, however, is overshadowed by the shear assessment challenge at intermediate support [8]. As can be seen from Figure 1, the pretension girders are designed with stands located in the flange to resist the sagging moment. Near the intermediate support, where the shear force and moment are maximum, the prestressing strands are located in the flexural compression zone, and it is currently unclear whether the presence of prestressing can be considered for shear assessment. Besides the prestressing effects, when assessed using the modern codes, the bridges constructed before 1974 lack sufficient shear reinforcement, and they often have non-code conforming shear and interface reinforcement detailing.

Due to the limited number of available studies on similar bridge types, the Guidelines for Assessment of Existing Bridges (RBK) [9] recommends disregarding the contribution of the prestress near the intermediate support. When assessing the bridges per the guideline, most bridges with limited shear reinforcement are found to be shear-critical. To investigate the aforementioned issues, a comprehensive experimental campaign is underway using full-scale replicas of the existing bridges. During the course of the experimental campaign, a blind prediction contest was organised to predict the response of two specimens. The details of the specimens were announced to the engineering community on January 25, 2023 [10]. The experimental results and contest winners were announced in a special session during the *fib* symposium 2023 in Istanbul. In this paper, we present the experimental observation of these two tests. In addition, the predictions of RBK[9], Model Code[2], and the second generation of Eurocode[11] are examined using the test results.

2 BLIND CONTEST EXPERIMENTS

2.1 Details of the Specimens

Specimens S10H1A and S10H2D, made by connecting two precast concrete beams with lengths of 11.25 m and 3.50 m, are selected for the contest. Both specimens share the same geometries and concrete mixture but have different reinforcement and strand layouts. Figure 2 presents details of the specimens, reinforcement and prestress layout. The longer beams of the two specimens have different strand layouts and prestress levels. Specimen S10H1A has a straight strand layout throughout the length, with individual strands pretensioned to 79.0 kN. A combination of straight and fan-shaped strand layout is used for specimen S10H2D with individual strands pretensioned to 118.5 kN. The short beams of both specimens are identical, and they have strands distributed across the entire depth with a pretension of 118.5 kN per strand. In addition to prestressing strands, steel reinforcements are provided for both longer beams.

To avoid shear failure outside the interest region, both specimens are provided with a closely spaced transverse reinforcement consisting of a diameter of 10 mm spaced at 150 mm. In the remaining region, a closed shear reinforcement with a diameter of 6 mm at 200 mm spacing is used. This results in a shear reinforcement ratio of 0.09 %, which is below the minimum shear reinforcement recommended by Eurocode and Model Code.

An inverted U-shape reinforcement is used at the interface between the prefab beams and the cast-in-situ topping (hereafter referred to as a Hairpin). While maintaining the same spacing of 200 mm, the diameter of the hairpin changed from 6 mm to 12 mm for specimens S10H1A and S10H2D, respectively. Consistent with the hairpin amount, topping reinforcement ratios of 1.16 % and 1.85 % are provided for specimens S10H1A and S10H2D, respectively (see Figure 2).

Special care was taken during the casting of the precast girders regarding the interface preparation. In the prefab factory, soon after the girders are cast, large aggregates with a maximum diameter of 32 mm are dispersed on the top surface of the precast beams to create a rough surface. The resulting interface can be categorised as a rough surface according to the definition of NEN-EN 1992-1-1 Eurocode 2 clause 6.2.5 (2) [1].

2.2 Material properties

C55/67 and C30/37 concrete grades are targeted for the precast girder and topping layer. The precast beams are cast using a self-compacting concrete mix with a maximum aggregate size of 16 mm, while normal-strength concrete with a similar aggregate size is used for the topping and cross beam.

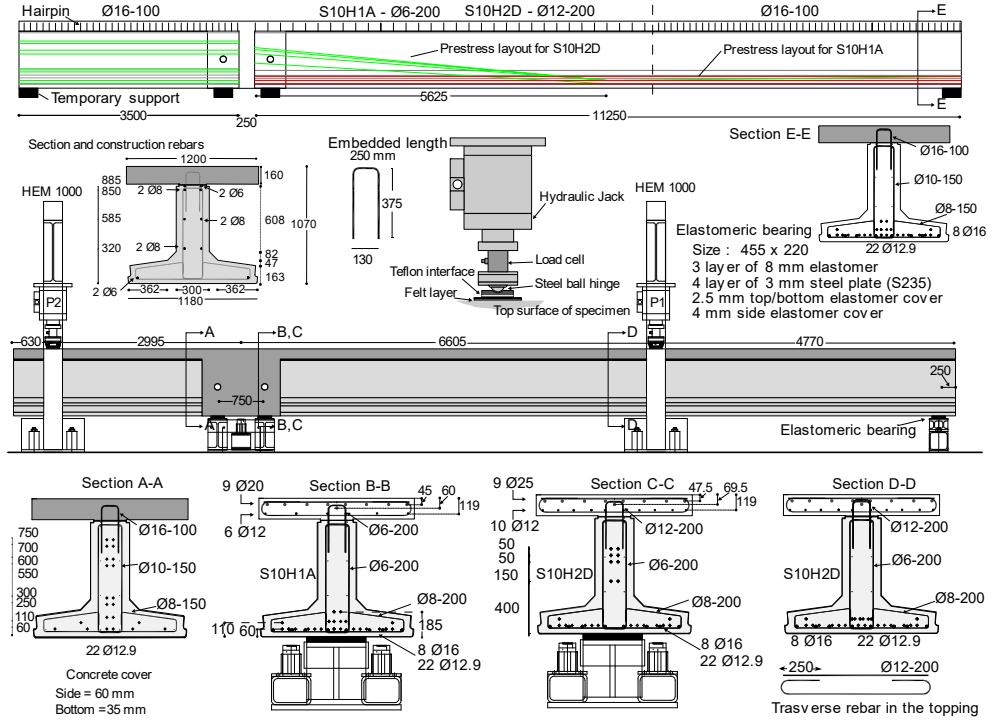


Fig. 2 Details of test specimens and test setup

The compressive strength of concrete at different ages was determined using 150 mm cube samples. Table 1 presents the average cubic strength of the concrete provided during the announcement of the blind contest. After the announcement, more cube samples were tested on experiment day. The compressive strengths of the precast girders S10H1A and S10H2D reached 97 and 84 MPa, and their corresponding cast in situ layer had compressive strengths of 64 MPa and 56 MPa.

Table 1 Average compressive strength of concrete

Specimen	Girder $f_{c,cube}$ [MPa]				ρ [kg/m ³]	Topping $f_{c,cube}$ [MPa]		ρ [kg/m ³]
	1 st day	7 th day	28 th day	Test day		28 th day	Test day	
S10H1A	-	63	77	97	2299	55	64	2333
S10H2D	39	-	76	84	2303	48	56	2324
Cantilever	42	66	75	-	2314	-	-	-

- Age of girder at connection: S10H1A - 84 days, S10H2D - 57 days, Cantilever - 64 days
- Age of girder at testing: S10H1A - 177 days, S10H2D - 247 days,

The precast beams are prestressed with a 7-wire prestressing strand (FeP 1860) with a diameter of 12.9 mm. For both specimens, steel rebars with a specified grade of B500B are used for the longitudinal and

shear reinforcement. Tables 2 provide the mechanical properties of the prestressing steel from the supplier. Due to space limitations, details of the lab test results of the reinforcing bar are not given here and they can be found in [10].

Table 2 Mechanical properties of prestressing strands.

Prestressing strand type	\varnothing [mm]	Nominal area [mm ²]	Tensile strength [MPa]	Elongation at maximum force [%]	Relaxation at 0.8 Fpu [%]
7-Wire	12.9	100	min 1860	min 3.5	max 4.5

2.3 Test setup, loading protocol and sensor plan

The boundary conditions of the experiment are given in Figure 2. The specimens are supported at the intermediate and end using elastomeric bridge bearings. The loads on the specimens are applied using two hydraulic jacks marked P_1 and P_2 . Steel loading plates with $300 \times 300 \times 20$ mm dimensions are used to introduce the force to the specimen. In both tests, jack P_1 was driven by displacement control loading with a constant loading rate of 0.02 mm/s. Jack P_2 was driven by force control loading. The magnitude of P_2 is based on the real-time reads of jack P_1 . A constant loading ratio of $P_1: P_2 = 1:0.63$ is maintained until shear failure. Although it did not occur, prior to the test, an alternative loading plan in the case of intermediate support yielding was also provided to the contest participants [10].

The sensor plan during the experiment was composed of conventional measurement techniques and advanced monitoring methods, including Digital image correlation (DIC), Fiber optics sensors, Smart aggregate, and Acoustic emission sensors. Due to the limited space, selected crack patterns using the DIC's principal strain and the tests' global response are presented here.

3 EXPERIMENTAL OBSERVATION

Both specimens failed in shear due to a loss of composite action between the precast girder and topping. Table 3 summarises the test results, and the observed behaviour of the tests is presented below.

Table 3 Summary of the experimental observation.

Specimen	$P_{1,ult}$ [kN]	$P_{2,ult}$ [kN]	δ_1^\ddagger [mm]	Prestress Loss [†] [%]
S10H1A	932	586	8.5	13
S10H2D	1947	1225	34.5	10

[†] *prestress loss evaluated using embedded fiber optics sensors* [12]

[‡] *Displacement the loading jack P_1*

The global response of specimen S10H1A is shown in Figure 3 (left). The first flexural cracks were initiated in the intermediate support region when the total load reached 650 kN. With the increase of the applied load, the flexural cracks start propagating from the topping to the web. The propagation of the flexural shear crack tip in the web was coupled with horizontal crack propagation along the interface. When the applied load reaches 1448 kN, a significant change in stiffness occurs from the flexural cracking of the girder under the loading jack P_1 . Soon after, the critical shear crack initiated from the interface at a load level of 1483 kN and propagated into the web and along the interface. The formation of the critical crack resulted in a sudden increase in interface opening and sliding. The ultimate capacity of the girder was soon reached at a total load of 1517 kN. A sudden drop in the applied load was observed due to the interface sliding and opening (see Figure 4a). Although the interface is cracked from the shear crack's root to the loading point P_1 , the applied load can be further increased to a secondary peak of 1850 kN, at which a brittle failure occurs due to web crushing under the loading point (see Figure 4b). Even though the girder has achieved a higher secondary peak, it cannot be considered the specimen's ultimate capacity. The localised concentrated clamping stress applied by the loading jack was essential for reaching the second peak by preventing interface sliding at the loading point. Given that similar crack-arresting mechanisms are improbable outside of laboratory conditions, the first peak should be selected as the girder's maximum capacity.

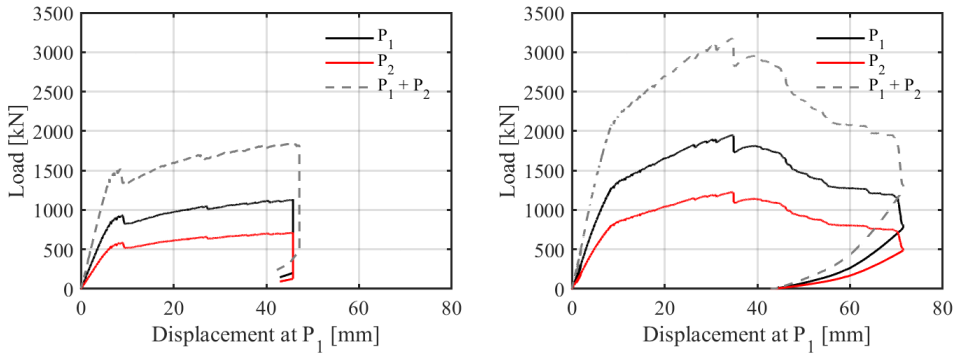


Fig. 3 Load displacement response: S10H1A (left), S10H2D (right)

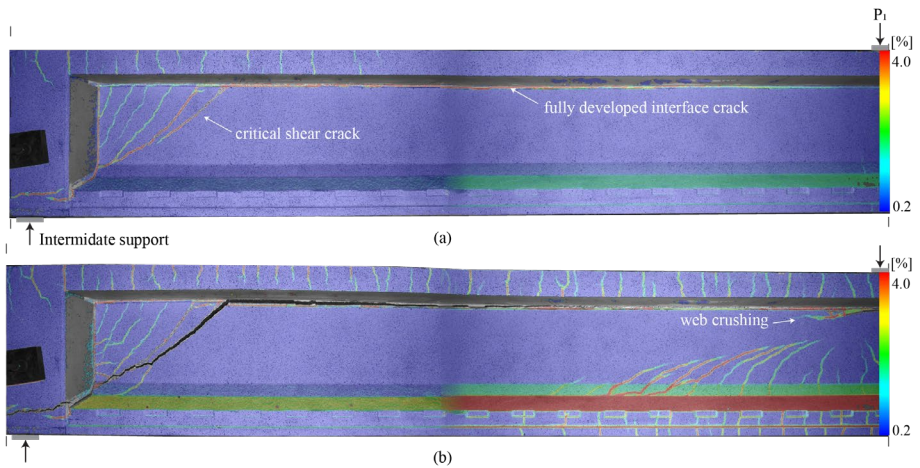


Fig. 4 Specimen S10H1A: (a) Immediate after the ultimate capacity (b) Second peak

The global load-displacement of specimen S10H2D is shown in Figure 3 (right). The first flexural crack was observed in the intermediate support at a total load of 489 kN. The subsequent loading resulted in the formation of additional flexural cracks and the propagation of several flexural shear cracks through the web. Similar to specimen S10H1A, the development of the crack tip in the interface is linked with the horizontal crack propagation of the crack root in the interface (see Figure 5a). Further loading has resulted in the propagation of the crack tip in the web and the initiation of closely spaced shear cracks from the interface. Significant stiffness change on the global response was observed at a load level of 2093 kN with flexural cracking at the loading point P_1 . Subsequent loading has resulted in the propagation and formation of new cracks in the region close to the support and the loading point P_1 . When the total load reaches 3171 kN, the ultimate capacity is reached due to a significant opening and sliding of the interface (see Figure 5b). Unlike specimen S10H1A, a second peak capacity was not observed in S10H2D. Additional loading in the post-peak stage has led to a significant interface opening with a global softening response.

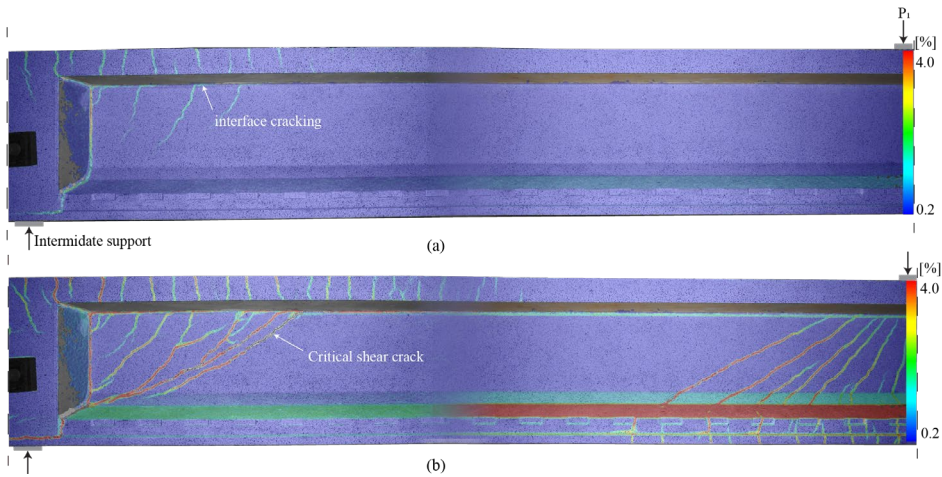


Fig. 5 Specimen S10H2D: (a) Total load – 1306 kN – flexural shear cracks developing through the web and interface (b) Cracking state at ultimate

4 COMPARISON WITH SELECTED CODE PROVISIONS

In this section, the experimental results of the contest specimens are used to examine the flexural shear capacity prediction RBK, Model Code, and FprEN 1992-1-1:2023 (Draft for the 2nd generation Eurocode 2). Due to space constraints, the other checks on the interface and shear tension capacity are not included. The following section initially briefly describes the code approaches, and then their prediction is discussed. Further details on the code formulations can be referred to from [2,9,11].

4.1 Brief description of selected codes

4.1.1 RBK

The Dutch RBK (RTD 1006:2022) [9] uses the general Eurocode2 expression for the flexural shear capacity provided by the concrete (see Equations 2). The concrete contribution is allowed to be added to the stirrups contribution for members with at least the minimum shear reinforcement. According to the guideline, the contribution of the prestress to the shear capacity should not be considered for the precast continuous girders. Therefore, when applying RBK for the current specimens, the influence of the prestress is ignored except for the vertical component of the fan layout.

$$V_{Rd,c,mean} = [0.163k_{cap} k (100\rho_l f_{ck})^{1/3} + 0.225\sigma_{cp}] b_w \text{gem} d_e \quad (2)$$

4.1.2 FprEN 1992-1-1:2023 (Draft for the 2nd generation Eurocode 2)

In the coming years, the second generation of Eurocode [11] is expected to be widely used to assess existing bridges. The code formulation uses Critical Shear Crack Theory (CSCT)[13] as a basis (see Eq 3). According to the code, the shear stress resistance is given in Equation 4. In addition, the code provides an approach for cases requiring more advanced verification (see Equation 5). Comparing Eq 3 and Eq 5, one may note that the main difference is the reference strain used for the shear capacity evaluation. In the base model, the reference strain is taken in the web, while the strain in longitudinal reinforcement is used in the detail verification. While both methods are feasible, when applied near the intermediate support region, it will become evident that the form used in the code cannot reflect the effect of prestress in the girder. In the current bridge system, only the girder is prestressed, and the prestressing does not directly affect the strain of the longitudinal reinforcement. In the following section, to properly reflect the effect of prestress, the shear capacity as per the second generation of Eurocode is done using the base model (Eq 3).

$$\frac{V_R}{bd\sqrt{f_c}} = \frac{1}{6} \frac{2}{1+120 \frac{\epsilon d}{16+d_g}} \quad \text{where : - } \epsilon \text{ at } 0.6d \text{ from the compression face} \quad (3)$$

$$\tau_{Rd,c} = \frac{0.66}{\gamma_v} \left(100 \rho_l f_{ck} \frac{d_{dg}}{d} \right)^{\frac{1}{3}} \geq \tau_{Rd,c,min} \quad (4)$$

$$\tau_{Rd,c} = 0.33 \frac{\gamma_{def}^{\frac{2}{3}} \sqrt{f_{ck}}}{\gamma_v^2 (1+24\gamma_{def} \epsilon_v \frac{d}{d_{dg}})} \quad \text{where : - } \epsilon_v \text{ is the strain at the longitudinal reinforcement} \quad (5)$$

4.1.3 Model Code 2020

The *fib* Model Code is an alternative strain-based shear model suitable for detail assessment. In the code, the shear assessment of existing structures should be done using a higher level of approximation. In Model Code 2010 [2], a shear formula based on the modified compression field theory was introduced for members without shear reinforcement, and it is also kept in the new MC2020[14](see Equation 6). In Eq 6, the code states the k_{dg} factor of two should be used if the member has a shear depth higher than 800 mm and concrete compressive strength greater than 70 MPa. This requirement produces a distinct jump at the concrete compressive strength of 70 MPa. For the current tests, the mean cylindrical strength of the girders was close to 70 MPa. To avoid unreasonable scatter between experiments with slight changes in compressive strength, two separate analyses, V_{MC1} and V_{MC2} , are done considering the mean cylindrical strength of 67 MPa and 70 MPa.

$$v_{Rd,c} = k_v \frac{\sqrt{f_{ck}}}{\gamma_c} b_w z_v, \quad k_v = \frac{0.4}{1+1500\epsilon_x} \frac{1300}{1000+k_{dg}z_v}, \quad k_{dg} = \frac{32}{16+d_g} \geq 0.75 \quad (6)$$

4.2 Code comparison and discussion

Generally speaking, the shear capacity evaluation using RBK is straightforward. In contrast, the strain-based approach requires an iterative approach in which the normal strain is evaluated at the reference layer, considering the effect of prestress and applied actions. The normal strain for the present composite members is determined by a nonlinear layered sectional analysis to properly consider the influence of prestress on the girder and the applied action on the entire section.

Table 4 presents the comparison between code prediction and experimental results of the specimens. All the codes provide safe and overly conservative predictions. Although the strain-based approaches can be used to consider the influence of prestress, no additional capacity is observed above the RBK prediction, in which the effect of prestress is ignored. From the selected codes, the Model Code provides the most conservative estimate when the concrete strength is 70 MPa. This is mainly attributed to the size effect component of Equation 6. A similar level of conservatism was also previously observed for large prestressed members with insufficient reinforcement [15]. Although it is not presented here, the code's prediction can be significantly enhanced if the size effect component of Eq 6 is ignored, as suggested in [15].

Table 4 Comparison of code prediction against experiment.

Specimen	V_u^* [kN]	V_{RBK} [kN]	V_{CSCT} [kN]	V_{MC1} [kN]	V_{MC2} [kN]	$\frac{V_u}{V_{RBK}^*}$	$\frac{V_u}{V_{CSCT}^*}$	$\frac{V_u}{V_{MC1}^*}$	$\frac{V_u}{V_{MC2}^*}$
S10H1A	541	371	275	341	261	1.82	2.77	2.02	2.88
S10H2D	1129	495 [†]	513 [†]	507 [†]	376 [†]	2.68	2.61	2.60	3.73

* Shear capacity reducing the shear force due to own weight at the critical location

† The shear capacity includes the vertical component of the prestress

‡ Own weight of the girder not included

5 CONCLUSIONS

In this paper, the experimental observation of two precast continuous girders that were part of the recent blind contest is presented. Both specimens failed in shear due to the opening of the interface between the precast girder and the topping layer. The study also examines the prediction of three standards that can be used for the assessment of existing bridges. The following conclusions are made based on the test observation and code comparison for the precast continuous girder at the intermediate support:-

- The interface behaviour between the topping and precast girder significantly affects the shear behaviour and ultimate capacity.
- The empirical (RBK) and state-of-the-art strain-based approaches provide safe yet overly conservative predictions.
- The conservative predictions from the current codes highlight the need for a tailored assessment method to avoid unnecessary intervention in these existing bridges.

Acknowledgements

The authors would like to thank all the researchers and practitioners for participating in this blind prediction contest and Rijkswaterstaat for supporting this research project.

References

- [1] CEN., 2005. Eurocode 2: Design of Concrete Structures—Part 1-1 General Rules and Rules for Buildings. NEN-EN 1992-1-1:2005. Brussels, Belgium, 229 pp: Comité Européen de Normalisation.
- [2] Fédération Internationale du Béton (fib), 2013. fib model code for concrete structures 2010. Lausanne: Ernst & Sohn;
- [3] Yang, Y., 2014. “Shear Behaviour of Reinforced Concrete Members without Shear Reinforcement A New Look at an Old Problem.” PhD Thesis, Delft University of Technology.
- [4] Lantsoght, E.O.L., 2013. “Shear in Reinforced Concrete Slabs under Concentrated Loads close to Supports.” PhD Thesis, Delft University of Technology.
- [5] Amir, S., 2014. “Compressive Membrane Action in Prestressed Concrete Deck Slabs.” PhD Thesis, Delft University of Technology.
- [6] Ensink, S., 2024. “SYSTEM BEHAVIOUR IN PRESTRESSED CONCRETE T-BEAM BRIDGES.” PhD Thesis, Delft University of Technology.
- [7] Roosen, M.A., 2021. “Shear failure of prestressed girders in regions without flexural cracks.” PhD Thesis, Delft University of Technology.
- [8] Ibrahim, M.S., Yang, Y., Roosen, M., Hendriks, M.A.N., 2022. Challenges on the shear behavior of existing continuous precast girder bridges. Proc. of the 14th fib International PhD Symposium in Civil Engineering,.
- [9] RBK 1.2.1 RTD 1006:2022., 2022. Guidelines for assessing works of art The Assessment Guidelines Works of Art (in Dutch). Utrecht, the Netherlands,.
- [10] Ibrahim, M.S., Kostense, N.W., Poliotti, M., Yang, Y., 2023. Home. <https://concrete-prediction-contest.tudelft.nl/home>. [accessed May 5, 2024].
- [11] CEN/TC 250/SC 2 N 2078., 2023. FINAL DRAFT FprEN 1992-1-1-Eurocode 2-Design of concrete structures-Part 1-1: General rules and rules for buildings, bridges and civil engineering structures.
- [12] Ibrahim, M., Poliotti, M., Yang, Y., Hendriks, M.A.N., 2023. Measurement of Restraint Moment Effect on Lab Specimens with Precast Girders Made Continuous. Lecture Notes in Civil Engineering, vol. 350 LNCE. Springer Science and Business Media Deutschland GmbH p. 846–55.
- [13] Muttoni, A., Ruiz, M.F., 2008. “Shear Strength of Members without Transverse Reinforcement as Function of Critical Shear Crack Width.” ACI Structural Journal: 163–72.
- [14] Fédération internationale du béton., 2023. fib Model Code for Concrete Structures (2020). Chemin du Barrage, Station 18, CH-1015 Lausanne.
- [15] Choi, J., Zaborac, J., Bayrak, O., 2021. “Assessment of shear capacity of prestressed concrete members with insufficient web reinforcement using AASHTO LRFD general shear design method.” Engineering Structures 242, Doi: 10.1016/j.engstruct.2021.112530.